NIH Public Access
Author Manuscript
J Periodontal Res. Author manuscript; available in PMC 2012 November 19.

Published in final edited form as:
J Periodontal Res. 2010 December ; 45(6): 748–756. doi:10.1111/j.1600-0765.2010.01295.x.

Type 1 diabetes predisposes to enhanced gingival leukocyte margination and macromolecule extravasation *in vivo*

C. Sima, **K. Rhourida**, **T. E. Van Dyke**, and **R. Gyurko**
Department of Periodontology and Oral Biology, Goldman School of Dental Medicine, Boston University, Boston, MA, USA

Abstract

Background and Objective—Diabetes predisposes to periodontal disease. However, the cellular and molecular mechanisms linking the two conditions are not clear. The impact of chronic hyperglycemia on leukocyte margination and macromolecule extravasation was determined in gingival vessels *in vivo*.

Materials and Methods—Gingival intravital microscopy was employed to measure extravasation of fluorescein isothiocyanate (FITC)–dextran in diabetic Akita and healthy wild-type (WT) mice. Rhodamine 6G and FITC–LY6G were injected for nonspecific and polymorphonuclear-specific leukocyte labeling, respectively. Surface expression of leukocyte adhesion molecules was determined with flow cytometry and western blotting.

Results—Vascular permeability was significantly increased in Akita gingival vessels compared with WT [permeability index (PI): WT, 0.75 ± 0.05; Akita, 1.1 ± 0.03: $p < 0.05$). Wild-type gingival vessels reached comparable permeability 2 h after intragingival injection of tumor necrosis factor α (TNFα), used here as positive control (PI, 1.17 ± 0.16). The number of rolling leukocytes was significantly elevated in diabetic gingiva (WT, 25 ± 3.7 cells/min; Akita, 42 ± 8.5 cells/min; $p < 0.03$). Similar rolling cell counts were obtained in WT after intragingival injection of TNFα (10 ng TNFα, 47 ± 1.3 cells/min; 100 ng TNFα, 57.5 ± 5.85 cells/min). The number of leukocytes firmly attached to the endothelium was similar in WT and Akita mice. Leukocyte cell-surface expression of P-selectin glycoprotein ligand-1 and CD11a was increased in Akita mice, while L-selectin remained unchanged when compared with WT. Moreover, P-selectin expression in Akita gingival tissues was elevated compared with that of WT.

Conclusion—Chronic hyperglycemia induces a proinflammatory state in the gingival microcirculation characterized by increased vascular permeability, and leukocyte and endothelial cell activation. Leukocyte-induced microvascular damage, in turn, may contribute to periodontal tissue damage in diabetes.

Keywords

diabetes; leukocyte; intravital microscopy; selectin; gingiva; microcirculation

Diabetes and chronic periodontal disease exhibit a bidirectional relationship centered on an enhanced inflammatory response manifested both locally and systemically. The severity and progression of periodontal tissue destruction in such conditions has been attributed to both bacterial and host contributions (1–6). Several studies have examined the impact of chronic

© 2010 John Wiley & Sons A/S

Robert Gyurko, DDS, PhD, 650 Albany Street, X343F, Boston University Medical Center, Boston, MA 02118, USA, Tel: 617-638-4774, Fax: 617 638 4799, gyurko@bu.edu.

$watermark-text
$watermark-text
$watermark-text

$watermark-text

$watermark-text

$watermark-text

hyperglycemia on periodontal structures and have demonstrated an enhanced innate inflammatory response leading to microvascular damage, extracellular matrix degradation and periodontal bone loss (5–9). Even though numerous epidemiological studies have confirmed that diabetes is a significant risk factor for periodontal disease, especially when poorly controlled, the mechanisms that link the two diseases are not fully understood.

In vivo examination of leukocyte behavior in postcapillary venules is essential for understanding the patho-biology of conditions associated with abnormal inflammatory responses such as Alzheimer's disease, inflammatory bowel disease, ischemia–reperfusion injury and diabetic complications, including periodontal disease (10,11). Development of accurate assessment technologies and reproducible methodologies to understand these spatial and temporal relationships *in vivo* has increased in recent years.

In order to characterize intravascular cell–cell interactions, new *in vitro* preparations, such as three-dimensional collagen gel matrices, monolayers of endothelial cells bathed with flowing solutions to mimic forces experienced by cells *in vivo*, and clusters of re-aggregated tissue fragments, have been developed. (12). Although they offer many advantages over previous assays, these models still lack intact blood and lymphatic vessels, which makes them unsuitable for investigation of leukocyte trafficking. Optical techniques offer cellular and even subcellular levels of resolution without *ex vivo* cell manipulation. Real-time imaging offers a powerful diagnostic tool for the evaluation of both endothelial cell and leukocyte functions in living organisms. Fluorescence video-microscopy using leukocyte-labeling dyes has been previously used to evaluate leukocyte behavior *in vivo* (12–17).

Gingival intravital microscopy is a noninvasive alternative that requires no surgical preparation to access the microvasculature, thereby eliminating false positive results due to surgical trauma and exposure of tissues to the outer environment. Furthermore, the preparation time is reduced and this eliminates sensitive steps that can introduce variability and make the technique less reproducible. The gingival marginal tissue in the labial mandibular interincisal area offers the advantage of superficially located postcapillary venules within a thin structure that can be easily observed using classic optical microscopic techniques combined with epifluorescence.

Mouse models for human diabetes have been used to understand the complex impact of prediabetic metabolic changes and chronic hyperglycemia on specific tissues *in vivo.* The Akita mouse is a model of type 1 diabetes with early-onset hyperglycemia. It is a heterozygote carrier of a missense point mutation in the *Ins*2 gene (C96Y), leading to synthesis of an abnormal pro-insulin peptide that progressively induces proteotoxicity and endoplasmic reticulum (ER) stress in the pancreatic β-cells, eventually leading to their apoptosis and hypoinsulinemia. Akita mice develop hyperglycemia as early as 4 wk of age. Males develop polyuria, polydipsia, polyphagia and neurological deficiencies at 8 wk of age (18,19) and show the first signs of nephropathy and retinopathy at 12 wk. The advantage of the Akita mouse over other models of diabetes is consistent high blood glucose levels without the complicating factors of obesity and autoimmune response against β-cells.

Leukocyte pre-activation or priming by diabetes has been demonstrated (20); however, the molecular mechanism by which chronic hyperglycemia leads to leukocyte activation is not known. The first step in leukocyte recruitment at sites of inflammation is mediated by selectins. The leukocyte cell surface ligand P-selectin glycoprotein ligand-1 (PSGL-1 or CD162) binds P-selectin (CD62P) on the surface of endothelial cells, leading to leukocyte rolling along endothelial surfaces. L-Selectin (CD62L) on leukocytes also contributes to neutrophil recruitment once initiated by P-selectin, although this may be primarily mediated by a ligand different from PSGL-1 (21). A recent review summarizes the roles of PSGL-1 in

$watermark-text

$watermark-text

$watermark-text

both margination and activation of leukocytes (22). Most importantly, the binding of P-selectin to PSGL-1 is absolutely required for activation of β2-integrins on leukocytes, notably LFA1 (CD11a/CD18), for slow rolling and attachment to endothelial cells (23).

The aim of the present study was to evaluate the impact of chronic hyperglycemia on early inflammatory vascular dynamics and leukocyte–endothelial cell interactions in the gingiva and to elucidate diabetes-induced changes in cell-surface molecules responsible for initiating leukocyte– endothelial adhesion. Since microvascular damage is a key step in the onset of diabetic complications, defining leukocyte–endothelial interactions in conditions of chronic hyperglycemia will further our understanding of periodontal inflammation in diabetes.

Material and methods

Mice and reagents

Akita mice on a C57BL/6 wild type (WT) background were obtained from Jackson Laboratories (Bar Harbor, ME, USA), aged 4–6 wk. Heterozygote Akita males and WTC57BL/6 females were bred in-house in a barrier facility and studied according to institutional and NIH guidelines. Adult mice (age 8–10 wk) of both sexes were used in experiments. All mouse experiments were in conformity with the standards of the Public Health Service Policy on Humane Care and Use of Laboratory Animals and were approved by the Institutional Animal Care and Use Committee of Boston University. Mice were fed standard laboratory chow and water *ad libitum*. Offspring were genotyped using ear samples that were further processed for PCR analysis. Hyperglycemic phenotype was confirmed by blood glucose measurement using a digital glucose meter (Accu-Check; Roche Diagnostics, Indianapolis, IN, USA).

Rhodamine 6G (R6G; Molecular Probes; Invitrogen, Carlsbad, CA, USA), fluorescein isothiocyanate–dextran (FITC–dextran; molecular weight, 150 kDa), Wright-Giemsa, zymosan A solution (Sigma-Aldrich, St. Louis, MO, USA), FITC-anti-LY6G, anti-PSGL1, anti-CD11a antibodies (BD Biosciences, San Jose, CA, USA), anti-P-selectin, anti-L-selectin antibodies (Santa Cruz, CA, USA) ketamine, xylazine, isoflurane, tumor necrosis factor α (TNFα; Roche Diagnostics), sterile saline solution (0.9% NaCl), phosphate-buffered saline (PBS; Invitrogen Life Technologies, Carlsbad, CA, USA), Bradford protein assay (Bio-Rad, Hercules, CA, USA), 5–0 silk surgical suture (Benco Dental, Pittston, PA, USA), FACScan flow cytometer and Cell Quest computer Software (Becton-Dickinson, Franklin Lakes, NJ, USA), FITC and tetramethylrhodamine isothiocyanate (TRITC) filter sets (Chroma Technology, Rockingham, VT, USA), luminal-enhanced chemiluminescence detection reagent (Cell Signaling Technology, Danvers, MA, USA), Zeiss Axiovert 200 inverted epifluorescent microscope equipped with a Sony DFW-X700 digital video camera, Sonycap (Sony Corporation, Tokyo, Japan) and Olympus MicroSuite software were obtained commercially, as indicated.

Intravital microscopy

Four- to 6-wk-old male mice weighing 20–25 g received 10 μL TNFα at different concentrations (1 or 10 μg/mL) intragingivally, between the two lower incisors, on the labial side of the alveolar process under brief isoflurane anesthesia.

One and a half hours later, mice were placed under a heating lamp for 20 min to induce vasodilatation, and then anesthetized with a mixture of ketamine (100 mg/kg body weight) and xylazine (10 mg/kg body weight) intraperitoneally. Body temperature was monitored with a rectal thermal probe. A 50 μL bolus of labeled fluorescent molecules (FITC–dextran + R6G or FITC–LY6G + R6G) in PBS was injected intravenously via one of the two side tail veins. A 5–0 silk suture was placed into the lower lip for retraction during microscopic

visualization of labial interincisal gingival, and the mouse was transferred onto a glass support plate and viewed under the inverted microscope. Gingival moisture was maintained with PBS at all times during the microscopic analysis. Single unbranched postcapillary venules (20–40 μm diameter, > 100 μm length) were selected for analysis. Pictures were captured, and several 30 s videos were recorded under the TRITC filter using ×40 magnification. At the end of the experiment mice were sacrificed with CO_2 according to the guideline of IACUC.

Vascular permeability

Micovascular permeability was measured using an approach published previously (24,25) with minor modifications based on the assumption of minimal plasma clearance of the tracer molecule in the interval between its intravenous administration and microscopic assessment. Thus, the initial fluorescence of the solute filling the vessel lumen and the plasma clearance constant for FITC–dextran (molecular weight 150 kDa) was not taken into account for calculation of permeability index (PI). We measured the initial change in fluorescence intensity as the solute moved across the vessel wall. Permeability was assessed on pictures taken under the green filter within 30 min after tracer molecule (FITC– dextran, 6 mg/kg) injection by calculating the green fluorescence intensity ratio in the extravascular (EV) vs. intravascular (IV) compartment. The average green intensity of 20 randomly selected pixels in the perivascular area within a 100 μm^2 area on each side of the vessel wall was calculated to determine the EV value. The same rule was applied for the intravascular compartment over 100 μm vessel length to determine the IV value. The PI was expressed as a ratio: PI = EV/IV, where EV and IV represent mean green intensity values for each compartment. Ratios were normalized to those of WT control animals, with higher values indicating an increase in FITC–dextran extravasation. (Fig. 1A,B).

Leukocyte margination

A 50 μL mixture of FITC–dextran (6 mg/kg, vasculature visualization) and rhodamine 6G (0.15 mg/kg, leukocyte *in vivo* labeling) in PBS were injected intravenously via one of the two side tail veins, and 30 s videos were recorded under the TRITC filter at ×40 magnification. Rolling and attached leukocytes were counted on the recorded videos. A 100 μm length of vessel was visualized, and cells moving along the vessel wall were considered rolling, while those that remained stationary for the 30 s observation period were considered attached (Fig. 1C).

To differentiate rolling and attached polymorphonuclear leukocytes (PMNs) from other leukocytes *in vivo*, a 50 μL mixture of FITC–LY6G (0.02 mg/kg, for PMN labeling) and R6G (0.15 mg/kg, for nonspecific leukocyte labeling) was injected via one tail vein. The merged pictures taken under the red and green filters show attached PMNs in yellow and rolling PMNs in green. The red-labeled cells indicate rolling leukocytes (Fig. 1D).

Isolated leukocytes from peritoneal cavity for fluorescence-activated cell sorting (FACS) analysis

Mice were injected intraperitoneally with 1 mL of zymosan A solution (1 mg/mL in PBS). Mice were killed after 2 h, and the abdominal skin was retracted to expose the abdominal muscles. Using a 22 gauge needle, 5 mL of sterile PBS was injected into the peritoneal cavity and then withdrawn to collect abdominal lavage fluid. Peritoneal leukocytes were centrifuged at 200 g for 10 min at room temperature, and cells were further washed with 1×PBS and centrifuged again as described above. Viable cells were counted in a hemocytometer using trypan blue exclusion and then resuspended to 10^6 cells/100 μL in cold FACS buffer (5% fetal bovine serum in PBS). Cells were incubated for 30 min in the dark with phycoerythrin (PE)- conjugated antibodies against PSGL-1, L-selectin and CD11a

$watermark-text $watermark-text $watermark-text

$watermark-text

$watermark-text

$watermark-text

at 4°C. Cells were washed once in FACS buffer, pelleted by centrifugation (200 *g* for 5 min at 4°C) resuspended in PBS, and fixed by adding 10% formalin in PBS. Flow cytometry was used to determine cell surface expression of the two target molecules. All flow cytometric data acquisition was performed on a FACScan flow cytometer. At least 10 000 events were collected per sample in all experiments. Data analysis was conducted using Cell Quest computer Software.

Western blotting

Under brief isoflurane anesthesia, gingival inflammation was induced in WT and Akita mice by injecting TNFα (100 ng) in PBS into each quadrant of the maxilla and mandible. Phosphate-buffered saline alone served as the control. Two hours later, mice were killed, and gingival tissue and blood were collected. Gingival tissue was homogenized using a mortar and pestle in liquid nitrogen. Lysis buffer was added to the tissues homogenate. Protein concentration was measured with the Bradford protein assay. Gingival protein extracts were boiled in Laemmle sample buffer, and 60 μg per lane were loaded on a 6% sodium dodecyl sulfate-polyacrylamide gel and electrophoresed at 120 V for 1 h. Proteins were transferred to a polyvinylidene fluoride membrane and incubated overnight with P-selectin antibody (1:200 dilution). Secondary antibody was applied for 2 h (1:5000 dilution). Protein bands were visualized with luminal-enhanced chemiluminescence detection reagent followed by autoradiography. Selectin levels were expressed as relative band intensity as determined by densitometry.

Statistical analysis

Student's unpaired *t*-test was used to compare measurements between WT and Akita mice. Flow cytometry data were analyzed using WinMDI 2.8 software, and mean fluorescence intensity values for WT and Akita cells were compared using Student's unpaired *t*-test. Values of $p < 0.05$ were considered statistically significant.

Results

Chronic hyperglycemia increases gingival vascular permeability

Vascular permeability in gingival postcapillary venules was measured using intravital microscopy 30 min after intravenous injection of FITC–dextran (6 mg/kg body weight). Fluorescence signal intensity measurement in intravascular and extravascular compartments revealed an increase in vascular permeability for large molecules in Akita mice compared with WT (Fig. 1A,B). Similar levels of vascular permeability can be induced in WT mice in 2 h after intragingival injection of 10 ng TNFα (Fig. 2).

Leukocyte rolling is increased in Akita gingival postcapillary venules

Circulating leukocytes were labeled intravenously by injecting R6G, a fluorescent dye that was shown to specifically stain white blood cells and platelets with no effect on leukocyte kinetics (26–28). The Ly6G surface antigen was used as a PMN-specific marker and stained with an FITC-bound anti-LY6G antibody as mentioned in the Material and methods section. The number of rolling leukocytes along the gingival endothelium of Akita mice was significantly increased compared with WT (WT, 25 ± 3.7 cells/min; Akita, 42 ± 8.5 cells/min; $n = 4$; $p < 0.05$). This rolling rate is comparable to what is observed in the 10 ng TNFα-injected WT mice (Fig. 3). The number of attached leukocytes, defined as R6G-positive cells that do not move in the 30 s observation period, was not significantly different between WT, Akita and WT+TNFα-injected mice (WT, 3.5 ± 5.1 cells/min; Akita, 0.66 ± 0.53 cells/min; WT+TNFα, 2.9 ± 0.33 cells/min). Double labeling with FITC–LY6G/R6G

indicated that the majority of attached leukocytes under TNFα stimulation are PMNs (Fig. 1C).

Chronic hyperglycemia enhances surface expression of adhesion molecules in leukocytes and endothelial cells

Flow cytometric analysis of leukocyte adhesion molecules was performed on zymosan A-elicited peritoneal leukocytes from WT and Akita mice. A marked increase of PSGL-1 was found in Akita leukocytes (Fig. 4A). In contrast, L-selectin levels were unchanged (Fig. 4B). Cell surface expression of the integrin subunit CD11a was elevated in Akita leukocytes (Fig. 4C). Endothelial expression of P-selectin was measured on protein extracts of gingival samples using western blotting. Akita gingival tissues expressed significantly more P-selectin compared with WT gingiva (Fig. 4D).

Discussion

The present study demonstrates that chronic hyperglycemia creates a microvascular environment in the gingiva that is in many aspects comparable to acute inflammation, including increased vascular permeability, increased leukocyte adhesion molecule expression and enhanced leukocyte rolling. A proinflammatory state is a well-established factor in the development of periodontal disease. The observation that hyperglycemia by itself, in the absence of additional inflammatory signals, promotes a proinflammatory environment indicates that diabetes is an independent risk factor for the development of periodontal disease (29–34).

One of the earliest events in inflammation is progressive vascular permeability for small molecules and later on for macromolecules, leading to osmotic changes and eventually edema. We measured vascular permeability changes under proinflammatory stimulation and in chronic hyperglycemia by comparing the outside–inside distribution of the tracer molecule (FITC–dextran) in nontreated Akita mice and intragingival TNFα-treated WT mice with healthy WT control animals. The results indicated a significant increase in gingival microvascular permeability for macromolecules in conditions of chronic hyperglycemia similar to an acute low-dose TNFα-induced gingival inflammation. Another study has reported increased microvascular permeability for FITC– dextran in a type 2 diabetes mouse model. Interestingly, the same study reports elevated serum levels of TNFα (9). The switch from a proinflammatory state mediated by TNFα to resolution of inflammation is essential for restoration of tissue homeostasis and prevention of chronic inflammation. There is growing evidence that periodontal disease involves a failure of resolution mechanisms to restore homeostasis (35).

Furthermore, we showed that PSGL-1 is overexpressed on the leukocyte surface of diabetic mice, while P-selectin expression in gingival endothelial cells is significantly increased in Akita compared with WT mice, indicating that hyperglycemia itself activates both leukocytes and endothelial cells. These findings correlate with our observation of increased leukocyte rolling along gingival microvessels in Akita mice, suggesting that a mechanism for a hyperglycemia-induced low level of gingival inflammation in diabetes may be the upregulation of adhesion molecules on both cell types. Our results indicate increased rolling and elevated CD11a surface expression in Akita gingival vessels but not increased firm attachment. This apparent discrepancy may be due to the fact that CD11a mediates firm attachment only when coupled with CD18, and the resulting integrin molecule LFA1 is in high-affinity conformation.

In order to control the level of inflammation and promote resolution, we need to clearly identify the molecular mechanisms that trigger the inflammatory response. In recent years,

$watermark-text $watermark-text $watermark-text

$watermark-text

$watermark-text

$watermark-text

extensive research has been conducted to understand the sequence of events and the connection between diabetes and inflammation (2,36–38). Hypertension and type 2 diabetes correlate in a systemic context marked by increased insulin resistance and elevated levels of high-sensitivity C-rective protein, which predict development of the metabolic syndrome. A recent study has reported significant microvascular alterations and increased leukocyte–endothelial cell interactions in UCP1/DTA prediabetic mice. This suggests phenotypic changes in leukocytes and endothelial cells early in the development of type 2 diabetes in the context of impaired glucose tolerance, obesity and dyslipidemia (39).

Chronic hyperglycemia itself induces low-grade inflammation via AGE– RAGE interactions (advanced glycation end-products and their receptors), which lead to induction of reactive oxygen species release by leukocytes and the upregulation of proinflammatory mediators and adhesion molecules (40–42). Based on *in vitro* flow chamber experiments, nuclear factor-κB and protein kinase C have been proposed to mediate leukocyte adhesion induced by hyperglycemia (43). Furthermore, impaired chemotaxis (44,45) and adherence (46,47) of neutrophils and delayed apoptosis have been reported in diabetic patients (8,48). Leukocyte–endothelial cell interactions have also been correlated with microvascular permeability increase indirectly via upregulation of intercellular adhesion molecule (ICAM-1) on endothelial cells (25) and directly via release of lytic factors that damage endothelial cells (49). These complex spatiotemporal correlations still remain to be investigated. We show in this study that chronic hyperglycemia induces overexpression of adhesion molecules in endothelial cells (P-selectin) and leukocytes (PSGL-1). The upregulation of P-selectin and its ligand PSGL-1 are prerequisites for leukocyte rolling and capture by endothelial cells (50). Furthermore, the CD11a part of LFA1 leukocyte-specific β2-integrin, which binds endothelial ICAM-1, leading to firm attachment prior to transmigration, was increased in Akita mice. This suggests that chronic hyperglycemia alters the leukocyte–endothelial cell interactions to favor increased rolling along gingival venules. Further, leukocyte surface overexpression of CD11a may explain in part the increased vascular permeability in Akita mice, considering its interaction with endothelial ICAM-1 and subsequent reorganization of the cytoskeleton and endothelial junctions. A recent study on the role of the cytoplasmic domain of PSGL-1 in leukocyte activation clearly showed that it mediates LFA1 activation via outside–in activation, thus indicating that increased P-selectin– PSGL-1 interaction may influence the endothelial cell cytoskeleton, with direct consequences for vascular permeability (23).

Taking a close look at these specific cell–cell interactions and their outcome *in vivo* is indispensable for validating and interpreting their meaning in the context of chronic diseases. The intravital microscopy technique for gingival microvascular visualization can be a useful tool for *in vivo* assessment of leukocyte–endothelial cell interactions and early events of the innate immune response to periodontal pathogens. Gingival video-microscopy gives further insight into the specificity of the inflammatory events in the oral cavity. By combining fluorescent labeling with gingival microscopy, we could identify the behavior of specific leukocyte subtypes during recruitment at sites of inflammation. Based on phenotypic features of different organs, these events are highly tissue specific, although they are part of the ‘nonspecific’ innate immune response (51). We were able to show that the gingival microvascular environment is changed in hyperglycemic conditions to favor a proinflammatory state (Fig. 5).

Overall, the present study shows a direct relationship between chronic hyperglycemia, increased leukocyte margination and macromolecule extravasation along gingival postcapillary venules *in vivo*. This chronic proinflammatory state induced by high blood glucose may contribute to the increased rate and severity of periodontal disease observed in people with diabetes.

$watermark-text

$watermark-text

$watermark-text

Acknowledgments

This work was supported by USPHS grants DE 16933 (R.G.) and DE15566 (T.E.V.D.) from the National Institute of Dental and Craniofacial Research, National Institutes of Health.

References

1. Van Dyke TE. The etiology and pathogenesis of periodontitis revisited. J Appl Oral Sci. 2009; 17:1.
2. Southerland JH, Taylor GW, Moss K, Beck JD, Offenbacher S. Commonality in chronic inflammatory diseases: periodontitis, diabetes, and coronary artery disease. Periodontol 2000. 2006; 40:130–143. [PubMed: 16398690]
3. Haffajee AD, Socransky SS. Microbiology of periodontal diseases: introduction. Periodontol 2000. 2005; 38:9–12. [PubMed: 15853934]
4. Socransky SS, Haffajee AD. Periodontal microbial ecology. Periodontol 2000. 2005; 38:135–187. [PubMed: 15853940]
5. Gapski R, Hasturk H, Van Dyke TE, et al. Systemic MMP inhibition for periodontal wound repair: results of a multi-centre randomized-controlled clinical trial. J Clin Periodontol. 2009; 36:149–156. [PubMed: 19207891]
6. Gyurko R, Siqueira CC, Caldon N, Gao L, Kantarci A, Van Dyke TE. Chronic hyperglycemia predisposes to exaggerated inflammatory response and leukocyte dysfunction in Akita mice. J Immunol. 2006; 177:7250–7256. [PubMed: 17082643]
7. Taubman MA, Valverde P, Han X, Kawai T. Immune response: the key to bone resorption in periodontal disease. J Periodontol. 2005; 76:2033–2041. [PubMed: 16277573]
8. Graves DT, Liu R, Alikhani M, Al-Mashat H, Trackman PC. Diabetes-enhanced inflammation and apoptosis – impact on periodontal pathology. J Dent Res. 2006; 85:15–21. [PubMed: 16373675]
9. Algenstaedt P, Schaefer C, Biermann T, et al. Microvascular alterations in diabetic mice correlate with level of hyperglycemia. Diabetes. 2003; 52:542–549. [PubMed: 12540633]
10. Bomboi G, Castello L, Cosentino F, Giubilei F, Orzi F, Volpe M. Alzheimer's disease and endothelial dysfunction. Neurol Sci. 2010; 31:1–8. [PubMed: 19838624]
11. Asaduzzaman M, Mihaescu A, Wang Y, Sato T, Thorlacius H. P-selectin and P-selectin glycoprotein ligand 1 mediate rolling of activated CD8+ T cells in inflamed colonic venules. J Investig Med. 2009; 57:765–768.
12. Cahalan MD, Parker I, Wei SH, Miller MJ. Real-time imaging of lymphocytes in vivo. Curr Opin Immunol. 2003; 15:372–377. [PubMed: 12900266]
13. Chiang EY, Hidalgo A, Chang J, Frenette PS. Imaging receptor microdomains on leukocyte subsets in live mice. Nat Methods. 2007; 4:219–222. [PubMed: 17322889]
14. Albertine KH, Gee MH. In vivo labeling of neutrophils using a fluorescent cell linker. J Leukoc Biol. 1996; 59:631–638. [PubMed: 8656047]
15. von Andrian UH. Intravital microscopy of the peripheral lymph node microcirculation in mice. Microcirculation. 1996; 3:287–300. [PubMed: 8930886]
16. Sumen C, Mempel TR, Mazo IB, von Andrian UH. Intravital microscopy: visualizing immunity in context. Immunity. 2004; 21:315–329. [PubMed: 15357943]
17. Kim MH, Curry FR, Simon SI. Dynamics of neutrophil extravasation and vascular permeability are uncoupled during aseptic cutaneous wounding. Am J Physiol Cell Physiol. 2009; 296:C848–C856. [PubMed: 19176758]
18. Yoshioka M, Kayo T, Ikeda T, Koizumi A. A novel locus, Mody4, distal to D7Mit189 on chromosome 7 determines early-onset NIDDM in nonobese C57BL/6 (Akita) mutant mice. Diabetes. 1997; 46:887–894. [PubMed: 9133560]
19. Asakawa A, Toyoshima M, Inoue K, Koizumi A. Ins2Akita mice exhibit hyperphagia and anxiety behavior via the melanocortin system. Int J Mol Med. 2007; 19:649–652. [PubMed: 17334640]
20. Karima M, Kantarci A, Ohira T, et al. Enhanced superoxide release and elevated protein kinase C activity in neutrophils from diabetic patients: association with periodontitis. J Leukoc Biol. 2005; 78:862–870. [PubMed: 16081595]

$watermark-text

$watermark-text

$watermark-text

21. Shigeta A, Matsumoto M, Tedder TF, Lowe JB, Miyasaka M, Hirata T. An L-selectin ligand distinct from P-selectin glycoprotein ligand-1 is expressed on endothelial cells and promotes neutrophil rolling in inflammation. Blood. 2008; 112:4915–4923. [PubMed: 18818390]
22. Zarbock A, Muller H, Kuwano Y, Ley K. PSGL-1-dependent myeloid leukocyte activation. J Leukoc Biol. 2009; 86:1119–1124. [PubMed: 19703898]
23. Miner JJ, Xia L, Yago T, et al. Separable requirements for cytoplasmic domain of PSGL-1 in leukocyte rolling and signaling under flow. Blood. 2008; 112:2035–2045. [PubMed: 18550846]
24. Sarelius IH, Kuebel JM, Wang J, Huxley VH. Macromolecule permeability of in situ and excised rodent skeletal muscle arterioles and venules. Am J Physiol Heart Circ Physiol. 2006; 290:H474–H480. [PubMed: 16126813]
25. Sumagin R, Lomakina E, Sarelius IH. Leukocyte-endothelial cell interactions are linked to vascular permeability via ICAM-1-mediated signaling. Am J Physiol Heart Circ Physiol. 2008; 295:H969–H977. [PubMed: 18641276]
26. Hickey MJ, Kanwar S, McCafferty DM, Granger DN, Eppihimer MJ, Kubes P. Varying roles of E-selectin and P-selectin in different microvascular beds in response to antigen. J Immunol. 1999; 162:1137–1143. [PubMed: 9916744]
27. Baatz H, Steinbauer M, Harris AG, Krombach F. Kinetics of white blood cell staining by intravascular administration of rhodamine 6G. Int J Microcirc Clin Exp. 1995; 15:85–91. [PubMed: 8655257]
28. Nolte D, Schmid P, Jager U, et al. Leukocyte rolling in venules of striated muscle and skin is mediated by P-selectin, not by L-selectin. Am J Physiol. 1994; 267:H1637–H1642. [PubMed: 7524368]
29. Graves DT, Cochran D. The contribution of interleukin-1 and tumor necrosis factor to periodontal tissue destruction. J Periodontol. 2003; 74:391–401. [PubMed: 12710761]
30. Hickey MJ, Kubes P. Intravascular immunity: the host-pathogen encounter in blood vessels. Nat Rev Immunol. 2009; 9:364–375. [PubMed: 19390567]
31. Hickey MJ, Reinhardt PH, Ostrovsky L, et al. Tumor necrosis factor-alpha induces leukocyte recruitment by different mechanisms in vivo and in vitro. J Immunol. 1997; 158:3391–3400. [PubMed: 9120299]
32. Hwa C, Sebastian A, Aird WC. Endothelial biomedicine: its status as an interdisciplinary field, its progress as a basic science, and its translational bench-to-bedside gap. Endothelium. 2005; 12:139–151. [PubMed: 16291517]
33. Pober JS, Sessa WC. Evolving functions of endothelial cells in inflammation. Nat Rev Immunol. 2007; 7:803–815. [PubMed: 17893694]
34. Medzhitov R. Origin and physiological roles of inflammation. Nature. 2008; 454:428–435. [PubMed: 18650913]
35. Van Dyke TE. Resolution of inflammation-unraveling mechanistic links between periodontitis and cardiovascular disease. J Dent. 2009; 37:S582–S583. [PubMed: 19501948]
36. Savoia C, Schiffrin EL. Vascular inflammation in hypertension and diabetes: molecular mechanisms and therapeutic interventions. Clin Sci (Lond). 2007; 112:375–384. [PubMed: 17324119]
37. Preshaw PM. Periodontal disease and diabetes. J Dent. 2009; 37:S575–S577. [PubMed: 19497655]
38. Lalla E, Lamster IB, Drury S, Fu C, Schmidt AM. Hyperglycemia, glycoxidation and receptor for advanced glycation endproducts: potential mechanisms underlying diabetic complications, including diabetes-associated periodontitis. Periodontol 2000. 2000; 23:50–62. [PubMed: 11276765]
39. Schaefer C, Biermann T, Schroeder M, et al. Early microvascular complications of prediabetes in mice with impaired glucose tolerance and dyslipidemia. Acta Diabetol. 2009 Epub ahead of print.
40. Chen YD, Xu X, Xia X, et al. MMP9 is involved in glycation end-products induced increase of retinal vascular permeability in rats and the therapeutic effect of minocycline. Curr Eye Res. 2008; 33:977–983. [PubMed: 19085380]
41. Wendt T, Bucciarelli L, Qu W, et al. Receptor for advanced glycation endproducts (RAGE) and vascular inflammation: insights into the pathogenesis of macrovascular complications in diabetes. Curr Atheroscler Rep. 2002; 4:228–237. [PubMed: 11931721]

42. Wong RK, Pettit AI, Quinn PA, Jennings SC, Davies JE, Ng LL. Advanced glycation end products stimulate an enhanced neutrophil respiratory burst mediated through the activation of cytosolic phospholipase A2 and generation of arachidonic Acid. Circulation. 2003; 108:1858–1864. [PubMed: 12963645]
43. Morigi M, Angioletti S, Imberti B, et al. Leukocyte-endothelial interaction is augmented by high glucose concentrations and hyperglycemia in a NF-kB-dependent fashion. J Clin Invest. 1998; 101:1905–1915. [PubMed: 9576755]
44. Waltenberger J, Lange J, Kranz A. Vascular endothelial growth factor-A-induced chemotaxis of monocytes is attenuated in patients with diabetes mellitus: a potential predictor for the individual capacity to develop collaterals. Circulation. 2000; 102:185–190. [PubMed: 10889129]
45. Golub LM, Nicoll GA, Iacono VJ, Ramamurthy NS. In vivo crevicular leukocyte response to a chemotactic challenge: inhibition by experimental diabetes. Infect Immun. 1982; 37:1013–1020. [PubMed: 6752017]
46. Andersen B, Goldsmith GH, Spagnuolo PJ. Neutrophil adhesive dysfunction in diabetes mellitus; the role of cellular and plasma factors. J Lab Clin Med. 1988; 111:275–285. [PubMed: 3343542]
47. Gilcrease MZ, Hoover RL. Neutrophil adhesion to endothelium following hyperosmolar insult. Diabetes Res. 1991; 16:149–157. [PubMed: 1802480]
48. Alba-Loureiro TC, Munhoz CD, Martins JO, et al. Neutrophil function and metabolism in individuals with diabetes mellitus. Braz J Med Biol Res. 2007; 40:1037–1044. [PubMed: 17665039]
49. Brown KA, Brain SD, Pearson JD, Edgeworth JD, Lewis SM, Treacher DF. Neutrophils in development of multiple organ failure in sepsis. Lancet. 2006; 368:157–169. [PubMed: 16829300]
50. Schmid-Schonbein GW. Analysis of inflammation. Annu Rev Biomed Eng. 2006; 8:93–131. [PubMed: 16834553]
51. Shapiro NI, Yano K, Sorasaki M, Fischer C, Shih SC, Aird WC. Skin biopsies demonstrate site-specific endothelial activation in mouse models of sepsis. J Vasc Res. 2009; 46:495–502. [PubMed: 19346756]

$watermark-text
$watermark-text
$watermark-text

$watermark-text
$watermark-text
$watermark-text

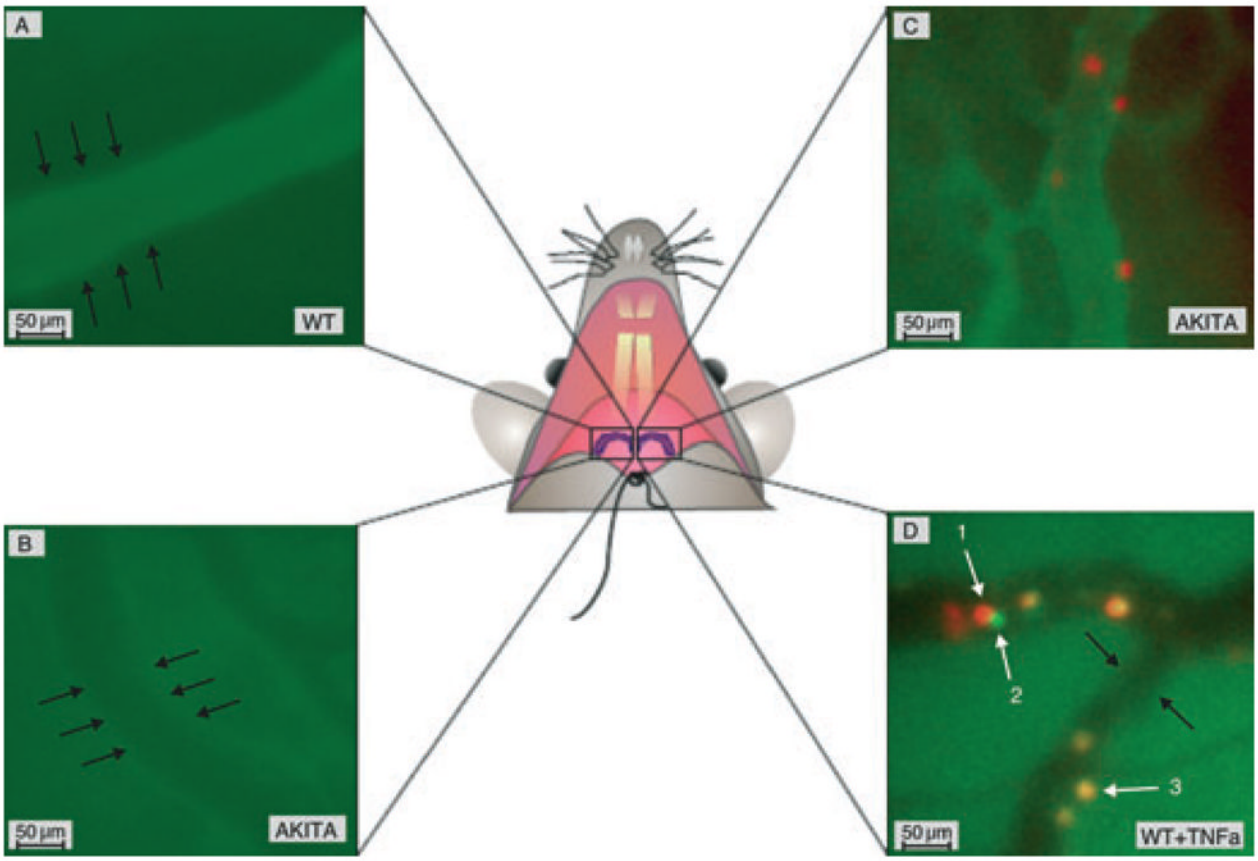

Fig. 1.

In vivo assessment of gingival vascular permeability and leukocyte margination. Rhodamine 6G (R6G; leukocyte labeling) and FITC– dextran (vasculature visualization and tracer molecule) or FITC–LY6G (PMN labeling) were injected intravenously, and intravital microscopy was performed at a controlled body temperature as specified in the Material and methods section. The black arrows indicate the outer side of the vessel wall. (A) The FITC–dextran is retained in the gingival vasculature of a WT mouse. (B) Increased FITC–dextran extravasation in Akita gingiva within the same time period. (C) Rhodamine 6G-positive leukocytes inside gingival postcapillary venules. The FITC–dextran (green) and R6G (red) images were merged offline to obtain this picture. (D) Overlapping images of R6G-positive (red) and LY6G-positive (green) cells indicate that the majority of leukocytes 2 h after tumor necrosis factor α (TNFα) stimulation are polymorphonuclear leukocytes (PMNs; yellow). The white arrows indicate intravascular leukocytes as follows: 1,rolling leukocyte (red); 2, rolling PMN (green); and 3, attached PMN (yellow). Scale bar represents 50 μm; original magnification ×400.

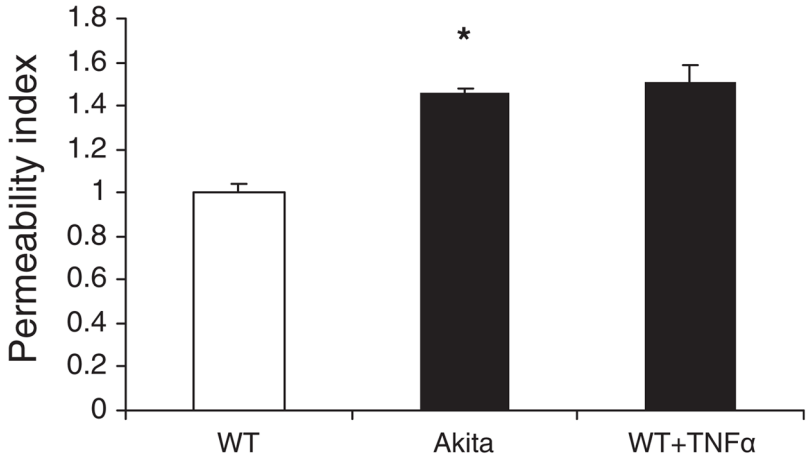

Fig. 2.

Microvascular permeability in the gingiva. Wild-type (WT) and Akita mice were injected with a 50 μL intravenous bolus of FITC–dextran (molecular weight, 150 kDa; 6 mg/kg), and 30 min later pictures were taken under the FITC filter. Tumor necrosis factor α (TNFα; 10 ng) was administered to some WT mice 2 h before the experiment. The permeability index represents the ratio of extravascular vs. intravascular green fluorescence intensity as specified in the Material and methods section. Permeability index values were normalized to WT control values. Results are means + SEM; $*p < 0.05$; $n = 3$ in each group.

$watermark-text
$watermark-text
$watermark-text

$watermark-text

$watermark-text

$watermark-text

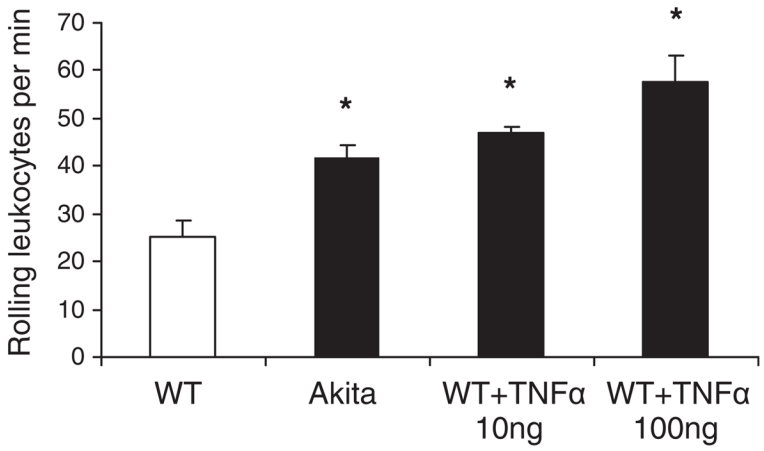

Fig. 3.

Leukocyte rolling in gingival venules. Leukocytes were labeled with an intravenous injection of R6G. A 100 μm segment of a superficial unbranched venule was selected, and intravital videos were recorded using a rhodamine filter. The number of R6G-labeled cells rolling along the endothelium was counted during the 30 s observation period. Akita gingival vessels displayed a significantly higher number of rolling leukocytes than WT. Stimulation with 10 ng TNFα in WT gingiva 2 h before the experiment resulted in a comparable elevation in leukocyte rolling. Results are means + SEM; $*p < 0.03$; $n = 4$ in each group.

$watermark-text
$watermark-text
$watermark-text

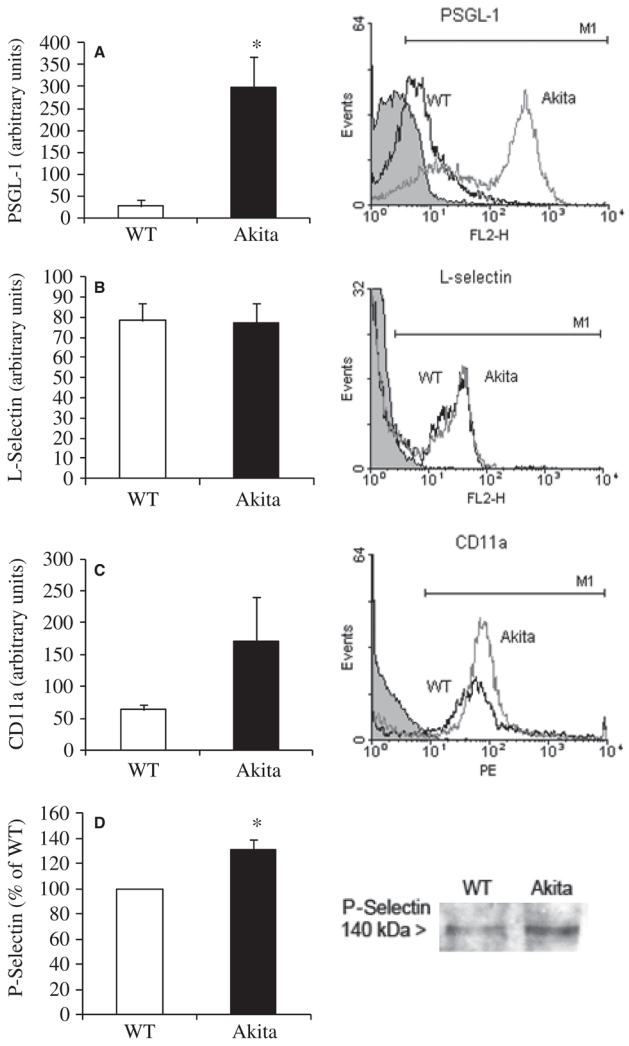

Fig. 4.

Leukocyte adhesion molecule expression in chronic hyperglycemia. (A) Flow cytometric analysis of peritoneal leukocytes showed increased surface expression of PSGL-1 ($n = 6$). (B,C) L-Selectin ($n = 7$) and CD11a ($n = 4$) expression ws not significantly different between WT and Akita leukocytes. Black line, WT; gray line, Akita: and black line with gray shaded area, IgG control. Representative histograms are shown on the left. (D) Densitometric analysis of P-selectin gingival expression assessed by western blot in Akita mice relative to WT. Data for P-selectin were normalized to total protein and expressed as a percentage of WT values ($n = 5$; $*p < 0.05$). FL2, orange fluorescence signal channel.

$watermark-text

$watermark-text

$watermark-text

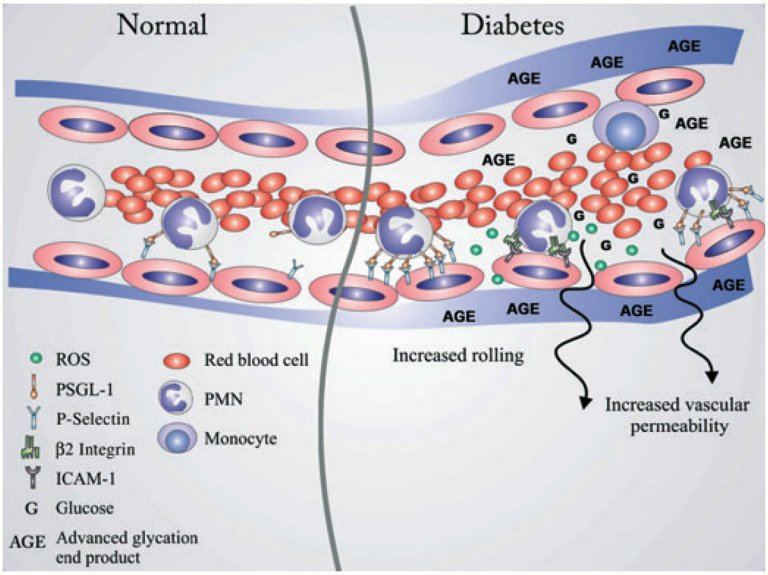

Fig. 5.

Leukocyte and vascular changes in chronic hyperglycemia. In physiological conditions, circulating leukocytes are constantly passing through narrow capillaries with smaller diameters than their own, resulting in direct contact with endothelial cells. This results in temporary rolling along the inner vessel wall via P-selectin–PSGL-1 interactions. In the postcapillary segment, they detach and continue circulating (left side, under ‘normal’). High blood glucose levels and the resulting advanced glycation end-products (AGEs) lead to both priming of leukocytes and endothelial cell changes which favor longer interaction between the two. We showed here that P-selectin on endothelial cells and its ligand PSGL-1 on leukocytes are overexpressed, which may in part explain the observed high rolling rate *in vivo*. Prolonged leukocyte–endothelial cell interaction may also promote release of reactive oxygen species (ROS) by polymorphonuclear leukocytes (PMNs) directly against the vessel wall by favoring both proximity and cell activation. Furthermore, changes in endothelial cell phenotype and the basement membrane structure may explain the increased permeability for large molecules (right side, under ‘diabetes’).